V. Govorukha · M. Kamlah

Analysis of an interface crack with multiple electric boundary conditions on its faces in a one-dimensional hexagonal quasicrystal bimaterial

Abstract An interface crack between dissimilar one-dimensional hexagonal quasicrystals with piezoelectric effect under anti-plane shear and in-plane electric loadings is considered. Mixed boundary conditions at the crack faces are studied. Using special representations of field variables via sectionally analytic vector-functions, a homogeneous combined Dirichlet–Riemann boundary value problem and a Hilbert problem are formulated. Exact analytical solutions of both these problems are obtained, and analytical expressions for the phonon and phason stresses and the electric field as well as for the derivative jumps of the phonon and phason displacements and also the electrical displacement jump along the bimaterial interface are derived. The field intensity factors are determined as well. The dependencies of the mentioned values on the magnitude and direction of the external electric loading and different ratios of electrically conductive and electrically permeable crack face zone lengths are demonstrated in graph and table forms.

Keywords Piezoelectric quasicrystals · Interface crack · Mixed electric conditions · Exact solution

1 Introduction

Quasicrystals (QCs), which were first discovered by Shechtman et al. [1], refer to a new class of functional and structural materials. They possess both quasiperiodic long-range translational order and noncrystallographic rotational symmetry, which are different from ordinary crystals and non-crystals. Due to their unique atomic structure, QCs have desirable physical, chemical and mechanical properties, such as high strength, low coef-ficient of friction, low adhesion, low electrical and thermal conductivity [2]. As a result of these meritorious properties, quasicrystalline materials are used more and more in the aerospace, automobile and nuclear fuel industries. On account of the engineering significance, the study of QCs has become an important branch of solid-state physics, materials science and solid mechanics.

Because of the quasiperiodic lattice structure of QCs, concepts of a high-dimensional space are introduced instead of the classical crystallographic theory. Two kinds of displacement fields are suggested to describe the elastic properties of QCs [3]. One is a phonon displacement field, which describes the lattice vibrations in QCs, and the other is a phason displacement field, which defines the quasiperiodic rearrangement of atoms. Corre-sponding to the phonon and phason displacement fields, there are phonon and phason stresses, respectively,

V. Govorukha (✉)
Department of Higher Mathematics, Physics and General Engineering Disciplines, Dnipro State Agrarian and Economic University, Serhii Efremov Str. 25, Dnipro 49600, Ukraine
e-mail: govorukhavb@yahoo.com

M. Kamlah
Institute of Applied Materials, Karlsruhe Institute of Technology, Hermann-Von-Helmholtz-Platz 1, 76344 Eggenstein-Leopoldshafen, Germany
e-mail: marc.kamlah@kit.edu

and they are coupled to each other. Depending on in how many directions the atom arrangement is quasiperiodic, QCs can be categorized into three classes, i.e., one-, two- and three-dimensional ones [4]. Generalized elasticity theory of QCs, material properties and convenient comprehensive reviews of the experimental and theoretical investigations are given in [5–10].

Many QCs possess piezoelectric effects. Due to this inherent electromechanical coupling, QCs are expected to be exploited in the design of smart devices like transducers, sensors and actuators. Theoretical foundations of the piezoelectricity of QCs were considered by Hu et al. [11] and Altay and Dömeci [12]. Taking advantage of the group representation theory, Li and Liu [13] and Rao et al. [14] investigated the physical properties of piezoelectric QCs. Zhang et al. [15] presented the internal and interfacial Green's functions of a one-dimensional quasicrystalline bimaterial with piezoelectric effect. A set of three-dimensional general solutions to static problems of one-dimensional hexagonal piezoelectric QCs was found by Li et al. [16] with use of two displacement functions. Li et al. [17] obtained fundamental solutions within the framework of thermo-electro-elasticity for an infinite/half-infinite space of one-dimensional hexagonal QCs. The general solution of the governing equations of plane elasticity of one-dimensional orthorhombic piezoelectric QCs was expressed by Zhang et al. [18] in terms of four potential functions. By utilizing the Stroh formalism and Green's function, Xu et al. [19] obtained the solutions of two-dimensional decagonal QCs with piezoelectric effect subjected to multi-field loads. Guo and Pan [20] proposed and analyzed a three-phase cylinder model for composites of piezoelectric QCs.

Experiments have shown that piezoelectric QCs are quite brittle and contain many micro-defects such as cracks which reduce their strength. Therefore, it is important to understand and be able to analyze the fracture characteristics of quasicrystalline structures so that reliable service life predictions of the pertinent devices can be conducted. Nowadays, the crack problems in homogeneous piezoelectric QCs got due attention in the literature. Fan et al. [21] obtained the fundamental solutions of three-dimensional cracks in one-dimensional hexagonal piezoelectric QCs. A penny-shaped dielectric crack in the quasicrystalline plate of the same structure was considered by Zhou and Li [22]. Using complex variable functions and operator techniques, Yu et al. [23] presented solutions of plane problems in one-dimensional piezoelectric quasicrystals, and, as an application, used the semi-inverse method to consider a mode-III stationary crack. Zhou and Li [24, 25] utilized the integral equation approach to obtain the exact solution of two symmetrically distributed collinear mode-III cracks parallel to and normal to the surface of a one-dimensional hexagonal piezoelectric quasicrystalline strip. Under electrically impermeable, permeable and limited permeable conditions, Yang and Li [26, 27] and Yang et al. [28] studied an anti-plane shear problem of a circular hole with a straight crack and an elliptical hole with two collinear cracks in one-dimensional hexagonal piezoelectric QCs. The problem of a Yoffe-type moving crack in one-dimensional hexagonal piezoelectric QCs was studied by Zhou and Li [29] under the action of anti-plane mechanical loading and in-plane electric loading. Explicit expressions for the field components of a moving non-constantly loaded anti-plane single crack embedded in an infinite region and within a half-space of one-dimensional hexagonal piezoelectric QCs were determine by Tupholme [30, 31].

It is worth to note that all mentioned results were performed for cracks in homogeneous piezoelectric QCs. On the other hand, the problem of an interface crack between dissimilar piezoelectric QCs, in spite of its importance, has not obtained due attention in the literature because of its complexity. In this respect, we can only mention a very restricted number of papers. Zhao et al. [32] and Dang et al. [33] gave a theoretical and numerical analysis of a three-dimensional arbitrarily shaped interface crack in a one-dimensional hexagonal thermo-electro-elastic quasicrystal bimaterial. A crack between dissimilar one-dimensional hexagonal piezoelectric QCs with electrically permeable and impermeable conditions at the crack faces under anti-plane shear and in-plane electric loadings was studied by Hu et al. [34]. A plane problem for an electrically permeable interface crack in one-dimensional piezoelectric QCs was analyzed analytically by Loboda et al. [35]. Recently, Hu et al. [36] considered the interaction of collinear interface cracks between dissimilar one-dimensional hexagonal QCs with piezoelectric effect under anti-plane shear and in-plane electric loadings.

Smart electronic devices are often constructed with use of the thin film electrodes or conducting layers embedded at some part of the material interface. Such electrodes generally can be considered as metal foils, which are more flexible than the surrounding piezoelectric quasicrystalline materials. In many cases, the mentioned loadings can induce an incompatible strain field, which may lead to delamination of electrodes and appearance of electrically conducting interface cracks. Within purely piezoelectric media, in which no phason fields are present, many analyses of electrically conducting interface cracks were undertaken [37–39]. However, electrically conducting interface cracks in bimaterial and multi-material components between dissimilar piezoelectric QCs have not been sufficiently studied till now. Motivated by this, in the present paper, a partially electroded interface crack between two dissimilar piezoelectric QCs subjected to external anti-plane shear and in-plane electric loadings is considered. An exact analytical solution of the full-fields in the cracked bimaterial is derived. It should be noted that the solution of the correspondent problem is important for practice, and it is mathematically much more complicated than for a completely electrically conducting interface crack. Stresses as well as displacements in the phonon and the phason fields and the electric fields are obtained in closed form. The field intensity factors and the crack faces sliding displacement are also derived and some conclusions from the obtained solution are discussed.

2 Basic equations for piezoelectric quasicrystals

In the absence of body forces and free electric charges, the basic equations for piezoelectric QCs presented, for example, by Altay and Dömeci [12] include

the constitutive equations

$$\sigma_{ij} = C_{ijkl}\varepsilon_{kl} + R_{ijkl}\omega_{kl} - e_{kij}E_k,\ H_{ij} = R_{klij}\varepsilon_{kl} + K_{ijkl}\omega_{kl} - d_{kij}E_k,\ D_i = e_{ijk}\varepsilon_{jk} + d_{ijk}\omega_{jk} + \lambda_{ij}E_j, \quad (1)$$

the equilibrium equations

$$\sigma_{ij,j} = 0,\ H_{ij,j} = 0,\ D_{i,i} = 0 \quad (2)$$

and the gradient equations

$$\varepsilon_{ij} = \frac{1}{2}\left(u_{i,j} + u_{j,i}\right), \omega_{ij} = w_{i,j},\ E_i = -\varphi_{,i}, \quad (3)$$

where $i,\ j,\ k,\ l = 1,\ 2,\ 3$; σ_{ij}, ε_{ij} and u_i are the components of the stresses, strains and displacements of the phonon field, respectively; H_{ij}, ω_{ij} and w_i are the components of the stresses, strains and displacements of the phason field, respectively; D_i, E_i and φ are the electric displacements components, the electric fields components, and the electric potential, respectively; C_{ijkl} and K_{ijkl} are the elastic constants of the phonon and phason fields, respectively; R_{ijkl} are the phonon–phason coupling elastic constants; e_{ijk} and d_{ijk} are the piezoelectric constants of the phonon and phason fields, respectively, and λ_{ij} are the dielectric permittivities. Repeated indices imply summation (from 1 to 3) and the subscript comma denotes partial derivative with respect to the rectangular Cartesian coordinates x_i $(i = 1,\ 2,\ 3)$.

In this paper, we will focus our attention on one-dimensional hexagonal piezoelectric quasicrystal medium of a point group *6 mm*, which has the $(x_1,\ x_2)$-plane as its isotropic periodic plane and the positive x_3-axis as its quasiperiodic poling direction.

Let the piezoelectric QCs be subject to combined anti-plane mechanical and in-plane electric loadings with reference to the $(x_1,\ x_2)$-plane. In this case, only the displacement u_3 of the phonon field, the displacement w_3 of the phason field and the electric potential ϕ, which are independent of x_3, will not vanish, i.e.,

$$u_1 = u_2 = 0,\ u_3 = u_3(x_1,\ x_2),\ w_1 = w_2 = 0,\ w_3 = w_3(x_1,\ x_2),\ \varphi = \varphi(x_1,\ x_2),$$

and the basic Eqs. (1–3) for the anti-plane problem of one-dimensional hexagonal piezoelectric QCs can be simplified as [23]

$$\sigma_{3m} = 2C_{44}\varepsilon_{3m} + R_3\omega_{3m} - e_{15}E_m,\ H_{3m} = 2R_3\varepsilon_{3m} + K_2\omega_{3m} - d_{15}E_m,$$

$$D_m = 2e_{15}\varepsilon_{3m} + d_{15}\omega_{3m} + \lambda_{11}E_m, \quad (4)$$

$$\sigma_{3m,m} = 0,\ H_{3m,m} = 0,\ D_{m,m} = 0, \quad (5)$$

$$\varepsilon_{3m} = \frac{1}{2}u_{3,m},\ \omega_{3m} = w_{3,m},\ E_m = -\varphi_{,m},\ m = 1, 2. \quad (6)$$

Substituting the gradient Eqs. (6) into the constitutive Eqs. (4), then into the equilibrium Eqs. (5), we get that the functions u_3, w_3 and ϕ satisfy the equations

$$\nabla^2 u_3 = 0, \quad \nabla^2 w_3 = 0, \quad \nabla^2\varphi = 0 \quad (\nabla^2 = \partial^2/\partial x_1^2 + \partial^2/\partial x_2^2),$$

i.e., they are harmonic. Therefore, according to the theory of complex variable function, u_3, w_3 and ϕ can be represented as the real parts of three arbitrary analytic functions $f_i(z)$ $(i = 1, 2, 3)$ of the complex variable $z = x_1 + ix_2$, such that

$$u_3 = 2\mathrm{Re} f_1(z),\ w_3 = 2\mathrm{Re} f_2(z),\ \varphi = 2\mathrm{Re} f_3(z), \tag{7}$$

where 'Re' denotes the real part of an analytic function, and $i = \sqrt{-1}$.

Introducing further the generalized displacement vector-function

$$\mathbf{u} = [u_3,\ w_3,\ \varphi]^T,$$

the relations (7) can be written in the form

$$\mathbf{u} = \mathbf{A}\mathbf{f}(z) + \bar{\mathbf{A}}\bar{\mathbf{f}}(\bar{z}), \tag{8}$$

where $\mathbf{f}(z) = [f_1(z),\ f_2(z),\ f_3(z)]^T$, $\mathbf{A}$ is a 3×3 unit matrix.

From Eqs. (4), (6), and (8), the generalized stresses vector-function

$$\mathbf{t} = [\sigma_{32},\ H_{32},\ D_2]^T$$

can also be expressed in the analytic functions form as

$$\mathbf{t} = \mathbf{B}\mathbf{f}'(z) + \bar{\mathbf{B}}\bar{\mathbf{f}}'(\bar{z}), \tag{9}$$

where $f'(z) = \left[f_1'(z),\ f_2'(z),\ f_3'(z)\right]^T$, and B is 3×3 matrix defined as

$$\mathbf{B} = i\begin{bmatrix} C_{44} & R_3 & e_{15} \\ R_3 & K_2 & d_{15} \\ e_{15} & d_{15} & -\lambda_{11} \end{bmatrix}.$$

Here and afterward, the superscript 'T' denotes transposition of a matrix, the overbar stands for the complex conjugate and a prime (') implies the derivative with respect to the associated arguments.

The representations (8) and (9) are convenient for the fracture analysis based on the extended Stroh formalism, but for the following analysis connected with an electrically conducting interface crack it is useful to introduce the new vector-functions

$$\mathbf{v} = \left[\frac{\partial u_3}{\partial x_1},\ \frac{\partial w_3}{\partial x_1},\ D_2\right]^T,\ \ \mathbf{p} = [\sigma_{32},\ H_{32},\ E_1]^T.$$

Using the relations (8) and (9), these vector-functions can be represented in the form

$$\mathbf{v} = \mathbf{M}\mathbf{f}'(z) + \bar{\mathbf{M}}\bar{\mathbf{f}}'(\bar{z}) \tag{10}$$

$$\mathbf{p} = \mathbf{N}\mathbf{f}'(z) + \bar{\mathbf{N}}\bar{\mathbf{f}}'(\bar{z}) \tag{11}$$

where the matrices M and N are defined by means of the reconstruction of the matrices A and B in the form

$$\mathbf{M} = \begin{bmatrix} 1 & 0 & 0 \\ 0 & 1 & 0 \\ ie_{15} & id_{15} & -i\lambda_{11} \end{bmatrix},\ \ \mathbf{N} = \begin{bmatrix} iC_{44} & iR_3 & ie_{15} \\ iR_3 & iK_2 & id_{15} \\ 0 & 0 & -1 \end{bmatrix}.$$

We now consider an analysis of a bimaterial compound, which consists of two piezoelectric quasicrystalline half-spaces $x_2 > 0$ and $x_2 < 0$ of different material properties. Performing the calculations presented in Appendix A, one arrives at the representations

$$\langle \mathbf{v}(x_1) \rangle = \mathbf{W}^+(x_1) - \mathbf{W}^-(x_1), \tag{12}$$

$$\mathbf{p}(x_1, 0) = \mathbf{G}\mathbf{W}^+(x_1) - \bar{\mathbf{G}}\mathbf{W}^-(x_1), \tag{13}$$

where the 3×3 matrix $\mathbf{G}$ is defined in Appendix A and the arbitrary vector-function $W(z) = [W_1(z),\ W_2(z),\ W_3(z)]^T$ is analytic in the whole complex plane, including the bonded parts of the bimaterial interface. Here and afterward the brackets $\langle ... \rangle$ denote the jump of the corresponding function over the bimaterial interface.

In this paper, we consider one-dimensional hexagonal piezoelectric QCs of a point group *6 mm* poled in the x_3-direction. For this case, the matrix $\mathbf{G}$ has the form

$$\mathbf{G} = \begin{bmatrix} ig_{11} & ig_{12} & g_{13} \\ ig_{21} & ig_{22} & g_{23} \\ g_{31} & g_{32} & ig_{33} \end{bmatrix}. \tag{14}$$

where all g_{kl} ($k,\ l = 1,\ 2,\ 3$) are real.

Consider an arbitrary vector $\mathbf{h} = [h_1,\ h_2,\ h_3]$ and its product $\mathbf{hp}(x_1,\ 0)$, which, using the relation (13), can be written as

$$\mathbf{hp}(x_1, 0) = \mathbf{hGW}^{+}(x_1) - \mathbf{h\bar{G}W}^{-}(x_1). \tag{15}$$

Furthermore, we assume that

$$\mathbf{h\bar{G}} = -\gamma \mathbf{hG}$$

where γ is a constant to be determined. Based on this condition, we arrive at an eigenvalues and eigenvectors problem for determining the constant γ and the vector h:

$$\left(\gamma \mathbf{G}^T + \bar{\mathbf{G}}^T\right)\mathbf{h}^T = 0. \tag{16}$$

The condition of existence of a nontrivial solution of the system (16) provides the equation for determining the eigenvalues:

$$\det\left(\gamma \mathbf{G}^T + \bar{\mathbf{G}}^T\right) = 0.$$

The roots of this equation are

$$\gamma_1 = \frac{1+\delta}{1-\delta},\ \ \gamma_2 = \frac{1}{\gamma_1},\ \ \gamma_3 = 1,$$

where

$$\delta = \sqrt{\frac{g_{31}(g_{12}g_{23} - g_{22}g_{13}) + g_{32}(g_{21}g_{13} - g_{11}g_{23})}{g_{33}(g_{11}g_{22} - g_{12}g_{21})}}.$$

The numerical analysis shows that for the considered kind of piezoelectric QCs the inequality $\delta^2 > 0$ holds true.

Knowing the eigenvalues γ_j ($j = 1,\ 2,\ 3$) of the system (16), we can find the corresponding eigenvectors $\mathbf{h}_j = \left[h_{j1},\ h_{j2},\ ih_{j3}\right]$, where the constants h_{j1}, h_{j3} are real and have the forms

$$h_{11} = \Lambda_1 h_{12},\ \ h_{21} = \Lambda_1 h_{22},\ \ h_{31} = -\frac{g_{23}}{g_{13}}h_{32},\ \ h_{13} = -\Lambda_2\delta h_{12},\ \ h_{23} = \Lambda_2\delta h_{22},\ \ h_{33} = 0,$$
$$\Lambda_1 = (g_{22}g_{31} - g_{21}g_{32})/\Lambda, \quad \Lambda_2 = (g_{11}g_{22} - g_{12}g_{21})/\Lambda, \quad \Lambda = g_{11}g_{32} - g_{12}g_{31},$$

while h_{j2} can be replaced by any real numbers.

Introducing the new functions

$$F_j(z) = \mathbf{h}_j\mathbf{GW}(z) = is_{j1}W_1(z) + is_{j2}W_2(z) + s_{j3}W_3(z)(j = 1, 2, 3), \tag{17}$$

having the same properties as $\mathbf{W}(z)$, we can rewrite the relation (15) as

$$\mathbf{h}_j\mathbf{p}(x_1, 0) = F_j^{+}(x_1) + \gamma_j F_j^{-}(x_1), \tag{18}$$

where

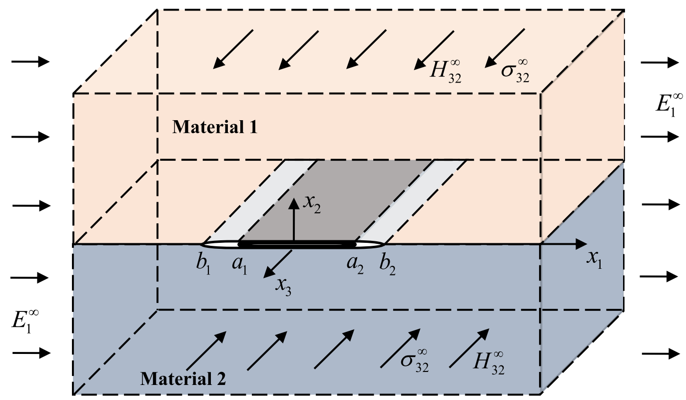

Fig. 1 An interface crack with mixed electrical boundary conditions between two dissimilar one-dimensional hexagonal piezoelectric QCs

$$s_{j1} = h_{j1}g_{11} + h_{j2}g_{21} + h_{j3}g_{31},\ \ s_{j2} = h_{j1}g_{12} + h_{j2}g_{22} + h_{j3}g_{32},\ \ s_{j3} = h_{j1}g_{13} + h_{j2}g_{23} - h_{j3}g_{33}.$$

From the relation (18), assuming $h_{j2} = 1$, we get the expression

$$h_{j1}\sigma_{32}(x_1, 0) + H_{32}(x_1, 0) + ih_{j3}E_1(x_1, 0) = F_j^+(x_1) + \gamma_j F_j^-(x_1)(j = 1, 2, 3) \tag{19}$$

for the combination of the phonon and phason stresses and the electric field at the bimaterial interface.

Using the relations (12) and (17), we can write the expression for the combination of the derivative jumps of the phonon and phason displacements and the electrical displacement jump over the bimaterial interface as

$$is_{j1}\langle u_3'(x_1)\rangle + is_{j2}\langle w_3'(x_1)\rangle + s_{j3}\langle D_2(x_1)\rangle = F_j^+(x_1) - F_j^-(x_1)(j = 1, 2, 3). \tag{20}$$

By means of the representations (19) and (20), the problems of linear relationship for one-dimensional piezoelectric quasicrystalline compounds with mixed boundary conditions at the bimaterial interfaces can be formulated and successfully solved.

3 Formulation of the problem

Consider a crack $b_1 \leq x_1 \leq b_2$ located at the interface $x_2 = 0$ between two dissimilar one-dimensional hexagonal piezoelectric quasicrystalline half-spaces $x_2 > 0$ and $x_2 < 0$ (Fig. 1). The upper and lower components of this bimaterial compound are piezoelectric QCs of a point group *6 mm*, which have a poling direction parallel to the x_3-axis and material properties $C_{44}^{(k)}$, $K_2^{(k)}$, $R_3^{(k)}$, $e_{15}^{(k)}$, $d_{15}^{(k)}$, and $\lambda_{11}^{(k)}$ ($k = 1$ stands for the upper half-space and $k = 2$ for the lower one).

We assume, that a part $L_a = (a_1,\ a_2)$ of the crack faces is electrically conducting and the remaining part $L_b = (b_1,\ a_1) \cup (a_2,\ b_2)$ is electrically permeable. Such situation can take place if the electrically conducting interface crack $(a_1,\ a_2)$ starts to propagate, i.e., increase its length to a certain value $(b_1,\ b_2)$. It is assumed also that there is no traction and free charge on the crack surface and the half-spaces are mechanically and electrically bonded along the bimaterial interface outside the crack. Thus, the interface crack problem must be solved under the following mixed boundary conditions in the plane $x_2 = 0$:

$$\sigma_{32}^{(1)} = \sigma_{32}^{(2)} = 0,\ H_{32}^{(1)} = H_{32}^{(2)} = 0,\ E_1^{(1)} = E_1^{(2)} = 0,\ x_1 \in L_a; \tag{21}$$

$$\sigma_{32}^{(1)} = \sigma_{32}^{(2)} = 0,\ H_{32}^{(1)} = H_{32}^{(2)} = 0,\ \langle D_2\rangle = 0,\ \langle E_1\rangle = 0,\ x_1 \in L_b; \tag{22}$$

$$\langle\sigma_{32}\rangle = 0,\ \langle H_{32}\rangle = 0,\ \langle u_3\rangle = 0,\ \langle w_3\rangle = 0,\ \langle D_2\rangle = 0,\ \langle E_1\rangle = 0,\ x_1 \notin (b_1, b_2). \tag{23}$$

The half-spaces are subjected to uniformly distributed shear phonon σ_{32}^{∞} and phason H_{32}^{∞} stresses as well as an electric field E_1^{∞} at infinity, which do not depend on the x_3 coordinate. This loading results in an anti-plane mechanical and in-plane electric state for which the relations (19) and (20) are valid.

Due to the method by which the relations (19) and (20) are constructed, they automatically satisfy the boundary conditions (23) at the bonded parts of the bimaterial interface and, accordingly, satisfy the conditions $\langle\sigma_{32}\rangle = 0$, $\langle H_{32}\rangle = 0$, $\langle E_1\rangle = 0$ at the crack faces. Satisfying the remaining boundary conditions (21) and (22) by means of (19), (20), we arrive at the equations

$$F_j^+(x_1) + \gamma_j F_j^-(x_1) = 0,\ x_1 \in L_a; \tag{24}$$

$$\mathrm{Re}\Big[F_j^+(x_1) + \gamma_j F_j^-(x_1)\Big] = 0,\ \mathrm{Re}\Big[F_j^+(x_1) - F_j^-(x_1)\Big] = 0,\ x_1 \in L_b. \tag{25}$$

The simultaneous satisfaction of both equalities (25) is possible only if the equation

$$\mathrm{Re} F_j^{\pm}(x_1) = 0,\ x_1 \in L_b \tag{26}$$

is valid.

Taking into account that the functions $F_j(z)$ are analytic in the whole complex plane cut along $L_a \cup L_b$ and that for $x_1 \notin (b_1, b_2)$ the relationships $F_j^+(x_1) = F_j^-(x_1) = F_j(x_1)$ are valid, it follows from (19)

$$\left(1 + \gamma_j\right) F_j(x_1) = h_{j1}\sigma_{32}(x_1, 0) + H_{32}(x_1, 0) + i h_{j3} E_1(x_1, 0) \text{ for } x_1 \to \infty.$$

Using that $\mathbf{p}(x_1, 0) = \left[\sigma_{32}^{\infty},\ H_{32}^{\infty},\ E_1^{\infty}\right]^T$ for $x_1 \to \infty$, one has from the last equation

$$F_j(z)\big|_{z\to\infty} = \frac{h_{j1}\sigma_{32}^{\infty} + H_{32}^{\infty} + i h_{j3} E_1^{\infty}}{1 + \gamma_j}. \tag{27}$$

4 Solution of the problem

Using the fact that $h_{33} = 0$, $s_{33} = 0$ and $\gamma_3 = 1$, the relations (24) and (26) lead to a homogeneous combined Dirichlet–Riemann problem

$$\Phi_k^+(x_1) + \gamma_k \Phi_k^+(x_1) = 0,\ x_1 \in L_a; \tag{28}$$

$$\mathrm{Im}\Phi_k^{\pm}(x_1) = 0, \quad x_1 \in L_b, \tag{29}$$

for the function $\Phi_k(z) = -i F_k(z)$, where $k = 1, 2$ and to the Hilbert problem

$$F_3^+(x_1) + F_3^-(x_1) = 0,\ x_1 \in (b_1, b_2), \tag{30}$$

for the function $F_3(z)$.

On base of (27) one can derive the conditions at infinity for the functions $\Phi_k(z)$ and $F_3(z)$

$$\Phi_k(z)|_{z\to\infty} = \frac{-i h_{k1}\sigma_{32}^{\infty} - i H_{32}^{\infty} + h_{k3} E_1^{\infty}}{1 + \gamma_k}, \tag{31}$$

$$F_3(z)|_{z\to\infty} = \frac{h_{31}\sigma_{32}^{\infty} + H_{32}^{\infty}}{2}. \tag{32}$$

Considering that $\gamma_2 = 1\big/\gamma_1$, the solution of the homogeneous combined Dirichlet–Riemann problem in question for $k = 2$ can be obtained from the associated solution for $k = 1$. Therefore, our attention will now be focused only on the case $k = 1$. The solution of such a problem concerning a rigid stamp was found by Nakhmein and Nuller [40] and, concerning an interface crack, it was developed by Govorukha et al. [41]. Using these results, an exact solution of the problem (28), (29), satisfying the condition at infinity (31) as well as the condition of the phonon and phason displacement uniqueness and the absence of an electric charge in the crack region, is found and presented in Appendix B.

The solution of the Hilbert problem (30) can be obtained by using the results of Muskhelishvili [42] as

$$F_3(z) = \frac{C_0 z + C_1}{\sqrt{(z - b_1)(z - b_2)}},$$

and after defining the arbitrary coefficients C_0 and C_1 from the conditions (32) at infinity and the condition

$$\int_{b_1}^{b_2} \left[F_3^+(x_1) - F_3^-(x_1)\right] \mathrm{d}x_1 = 0,$$

it takes the form

$$F_3(z) = \frac{h_{31}\sigma_{32}^{\infty} + H_{32}^{\infty}}{2}\left(z - \frac{b_1 + b_2}{2}\right)\frac{1}{\sqrt{(z - b_1)(z - b_2)}}. \tag{33}$$

Based on the obtained solutions (33), (B2) and the formulas (19), (20), the following equations for the field quantities at the different parts of the bimaterial interface are found.

for $x_1 > b_2$:

$$h_{11}\sigma_{32}(x_1, 0) + H_{32}(x_1, 0) = -\frac{1 + \gamma_1}{x_1 - d}\left[\frac{Q(x_1)\cos\phi(x_1)}{\sqrt{(x_1 - b_1)(x_1 - b_2)}} + \frac{P(x_1)\sin\phi(x_1)}{\sqrt{(x_1 - a_1)(x_1 - a_2)}}\right], \tag{34a}$$

$$h_{31}\sigma_{32}(x_1, 0) + H_{32}(x_1, 0) = \left(x_1 - \frac{b_1 + b_2}{2}\right)\frac{h_{31}\sigma_{32}^{\infty} + H_{32}^{\infty}}{\sqrt{(x_1 - b_1)(x_1 - b_2)}}, \tag{34b}$$

$$E_1(x_1, 0) = \frac{1 + \gamma_1}{h_{13}(x_1 - d)}\left[\frac{P(x_1)\cos\phi(x_1)}{\sqrt{(x_1 - a_1)(x_1 - a_2)}} - \frac{Q(x_1)\sin\phi(x_1)}{\sqrt{(x_1 - b_1)(x_1 - b_2)}}\right], \tag{35}$$

for $x_1 \in (a_1,\ a_2)$:

$$s_{11}\langle u_3'(x_1)\rangle + s_{12}\langle w_3'(x_1)\rangle = \frac{1 + \gamma_1}{\sqrt{\gamma_1}(x_1 - d)}\left[\frac{Q(x_1)\cos\phi^*(x_1)}{\sqrt{(x_1 - b_1)(b_2 - x_1)}} + \frac{P(x_1)\sin\phi^*(x_1)}{\sqrt{(x_1 - a_1)(a_2 - x_1)}}\right], \tag{36a}$$

$$s_{31}\langle u_3'(x_1)\rangle + s_{32}\langle w_3'(x_1)\rangle = -\left(x_1 - \frac{b_1 + b_2}{2}\right)\frac{h_{31}\sigma_{32}^{\infty} + H_{32}^{\infty}}{\sqrt{(x_1 - b_1)(b_2 - x_1)}}, \tag{36b}$$

$$\langle D_2(x_1)\rangle = \frac{1 + \gamma_1}{s_{13}\sqrt{\gamma_1}(x_1 - d)}\left[\frac{P(x_1)\cos\phi^*(x_1)}{\sqrt{(x_1 - a_1)(a_2 - x_1)}} - \frac{Q(x_1)\sin\phi^*(x_1)}{\sqrt{(x_1 - b_1)(b_2 - x_1)}}\right], \tag{37}$$

and for $x_1 \in (a_2,\ b_2)$:

$$s_{11}\langle u_3'(x_1)\rangle + s_{12}\langle w_3'(x_1)\rangle = \frac{2\cos[\pi h_2(x_1)]}{x_1 - d}\left[\frac{P(x_1)\sinh\left[\tilde{\phi}(x_1)\right]}{\sqrt{(x_1 - a_1)(x_1 - a_2)}} + \frac{Q(x_1)\cosh\left[\tilde{\phi}(x_1)\right]}{\sqrt{(x_1 - b_1)(b_2 - x_1)}}\right], \tag{38a}$$

$$s_{31}\langle u_3'(x_1)\rangle + s_{32}\langle w_3'(x_1)\rangle = -\left(x_1 - \frac{b_1 + b_2}{2}\right)\frac{h_{31}\sigma_{32}^{\infty} + H_{32}^{\infty}}{\sqrt{(x_1 - b_1)(b_2 - x_1)}}, \tag{38b}$$

$$E_1(x_1, 0) = \frac{2\sqrt{\gamma_1}\cos[\pi h_2(x_1)]}{h_{13}(x_1 - d)}\left\{\frac{P(x_1)\cosh\left[\tilde{\phi}(x_1) - \pi\varepsilon_1\right]}{\sqrt{(x_1 - a_1)(x_1 - a_2)}} + \frac{Q(x_1)\sinh\left[\tilde{\phi}(x_1) - \pi\varepsilon_1\right]}{\sqrt{(x_1 - b_1)(b_2 - x_1)}}\right\}, \tag{39}$$

where

$$\phi^*(x_1) = -Z^+(x_1)\left[\varepsilon_1\int_{a_1}^{a_2}\frac{\mathrm{d}t}{Z^+(t)(t - x_1)} + i\int_{b_1}^{a_1}\frac{h_1(t)\mathrm{d}t}{Z^+(t)(t - x_1)} + i\int_{a_2}^{b_2}\frac{h_2(t)\mathrm{d}t}{Z^+(t)(t - x_1)}\right],$$

$$\tilde{\phi}(x_1) = -iZ^+(x_1)\left(\varepsilon_1\int_{a_1}^{a_2}\frac{\mathrm{d}t}{Z^+(t)(t - x_1)} + i\int_{b_1}^{a_1}\frac{h_1(t)\mathrm{d}t}{Z^+(t)(t - x_1)} + i\int_{a_2}^{b_2}\frac{h_2(t)\mathrm{d}t}{Z^+(t)(t - x_1)}\right).$$

Relations (36a), (36b) and (38a), (38b) are the systems of two linear algebraic equations with respect to $\langle u_3'(x_1)\rangle$ and $\langle w_3'(x_1)\rangle$, from which these functions can be easily derived. Then, the crack faces sliding displacements can be found as

$$\langle u_3(x_1)\rangle = \int_{b_1}^{x_1} \langle u_3'(t)\rangle \mathrm{d}t,\ \ \langle w_3(x_1)\rangle = \int_{b_1}^{x_1} \langle w_3'(t)\rangle \mathrm{d}t.$$

It can be clearly seen that the field components of phonon stress, phason stress, electric field and electric displacement possess an inverse square root type singularity at the points a_k and b_k. Thus, we introduce the field intensity factors for the phonon and phason stresses

$$K_\sigma^{b_2} = \lim_{x_1\to b_2+0} \sqrt{2\pi(x_1-b_2)}\sigma_{32}(x_1,0),\ \ K_H^{b_2} = \lim_{x_1\to b_2+0} \sqrt{2\pi(x_1-b_2)}H_{32}(x_1,0),$$

and the electric field intensity factors

$$K_E^{a_2} = \lim_{x_1\to a_2+0} \sqrt{2\pi(x_1-a_2)}E_1(x_1,0),\ \ K_E^{b_2} = \lim_{x_1\to b_2-0} \sqrt{2\pi(b_2-x_1)}E_1(x_1,0).$$

Applying the formulas of Muskhelisvili [43] for Cauchy type integrals, which are expressed via the functions $\tilde{\varphi}(x_1)$, $\varphi^*(x_1)$ and $\varphi(x_1)$ in the vicinity of singular points a_2 and b_2, one arrives at

$$\phi(b_2)=0,\ \ \phi^*(a_2)=\pi,\ \ \tilde{\phi}(a_2)=\pi\varepsilon_1.$$

Solving the system (34a), (34b) and considering the obtained expressions in the vicinity of the point b_2, we arrive at the formulas for phonon and phason stress intensity factors

$$K_\sigma^{b_2} = -\frac{\sqrt{2\pi(b_2-b_1)}}{h_{11}-h_{31}}\left[\frac{1+\gamma_1}{(b_2-d)(b_2-b_1)}Q(b_2)+\frac{h_{31}\sigma_{32}^\infty+H_{32}^\infty}{2}\right], \tag{40}$$

$$K_H^{b_2} = \frac{\sqrt{2\pi(b_2-b_1)}}{h_{11}-h_{31}}\left[\frac{h_{31}(1+\gamma_1)}{(b_2-d)(b_2-b_1)}Q(b_2)+\frac{h_{11}\left(h_{31}\sigma_{32}^\infty+H_{32}^\infty\right)}{2}\right]. \tag{41}$$

Considering the expression (39) for $x_1\to a_2+0$ and for $x_1\to b_2-0$ leads to

$$K_E^{a_2} = \frac{-2\sqrt{2\pi}\gamma_1}{h_{13}(a_2-d)}\frac{P(a_2)}{\sqrt{(a_2-a_1)}}, \tag{42}$$

$$K_E^{b_2} = \sqrt{\frac{2\pi}{b_2-b_1}}\frac{(1-\gamma_1)Q(b_2)}{h_{13}(b_2-d)}. \tag{43}$$

Furthermore, we introduce

$$k_u = \lim_{x_1\to b_2-0}\sqrt{b_2-x_1}\langle u_3'(x_1)\rangle$$

and it is clear that the crack will be closed smoothly at the point b_2 if

$$k_u = 0.$$

Due to the formulas (38a) and (38b), the last equation can be written in the form

$$4s_{32}Q(b_2)+s_{12}(b_2-d)(b_2-b_1)\left(h_{31}\sigma_{32}^\infty+H_{32}^\infty\right)=0. \tag{44}$$

This equation gives a possibility to define the values of the external loading parameters for which the crack closes smoothly.

Table 1 Material properties of the one-dimensional hexagonal piezoelectric QCs [15]

	Upper material	Lower material
$C_{44}(10^9\text{Nm}^{-2})$	50	70.19
$K_2(10^9\text{Nm}^{-2})$	0.3	24
$R_3(10^9\text{Nm}^{-2})$	1.2	0.8846
$e_{15}(\text{Cm}^{-2})$	− 0.138	11.6
$d_{15}(\text{Cm}^{-2})$	− 0.16	1.16
$\lambda_{11}(10^{-9}\text{C}^2\text{N}^{-1}\text{ m}^{-2})$	0.0826	5

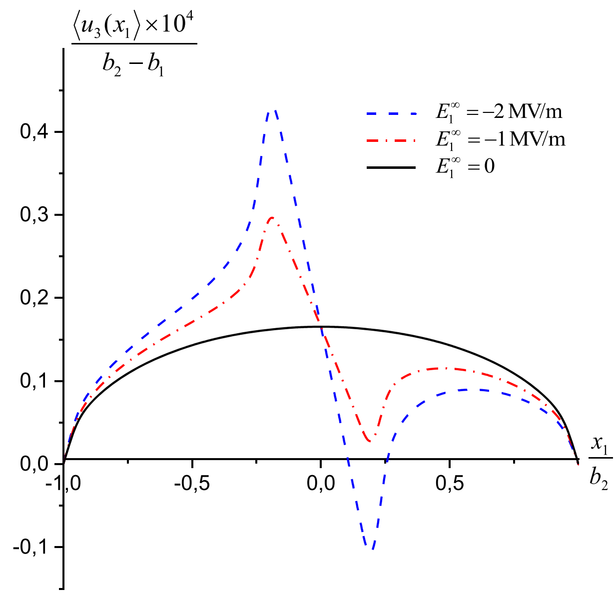

Fig. 2 The variation of the sliding displacement jump $\langle u_3(x_1)\rangle$ of the normalized phonon crack faces along the crack region for different values of E_1^∞

5 Numerical results and discussion

In this section, the selected numerical results are presented to analyze the fracture behavior of a partially electroded crack between two dissimilar one-dimensional hexagonal piezoelectric QCs. The main attention of the following numerical analysis will be devoted to the influence of the external electrical loading on the mechanical and electrical intensity factors as well as the variations of the field quantities at the bimaterial interface. The material properties of the QCs are listed in Table 1.

For the sake of clarity of the numerical illustrations it is assumed that the center of the interval (b_1, b_2) coincides with the origin. The positions of the points a_1 and a_2, determining the length of the electrically permeable zones, are defined by the parameters $\vartheta_1 = (a_1 - b_1)/(b_2 - b_1)$ and $\vartheta_2 = (b_2 - a_2)/(b_2 - b_1)$, respectively. Without loss of generality, the applied uniform phonon and phason stresses at far field are taken as $\sigma_{32}^\infty = 1$ MPa, $H_{32}^\infty = 0$.

The variation of the normalized crack faces sliding displacement jump for the phonon and phason fields, i.e., the jump functions $\langle u_3(x_1)\rangle$ and $\langle w_3(x_1)\rangle$ along the crack region (b_1, b_2), for different electric field loadings and $\vartheta_1 = \vartheta_2 = 0.4$ are calculated and presented in Figs. 2 and 3, respectively. It is clearly seen from these results that for $E_1^\infty = 0$ the jump of the functions $\langle u_3(x_1)\rangle$ and $\langle w_3(x_1)\rangle$ have symmetrical behavior. However, the deviation of E_1^∞ from zero leads to a cardinal distortion of the curves and their fast variation at the points a_1 and a_2, dividing the electrically conducting and electrically permeable crack face regions. Moreover, it shows that the maximum of the curves increases as the electric field loading increases. It is worth to be mentioned also that the change of the sign of electric field loading E_1^∞ will lead to mirror mapping of the obtained graphs with respect to the x_2-axis.

The variation of $\langle u_3(x_1)\rangle$ in the left neighboring area of the point b_2 is shown in Fig. 4. Numerical results are obtained for the same geometrical characteristics as before and various values of E_1^∞. The value

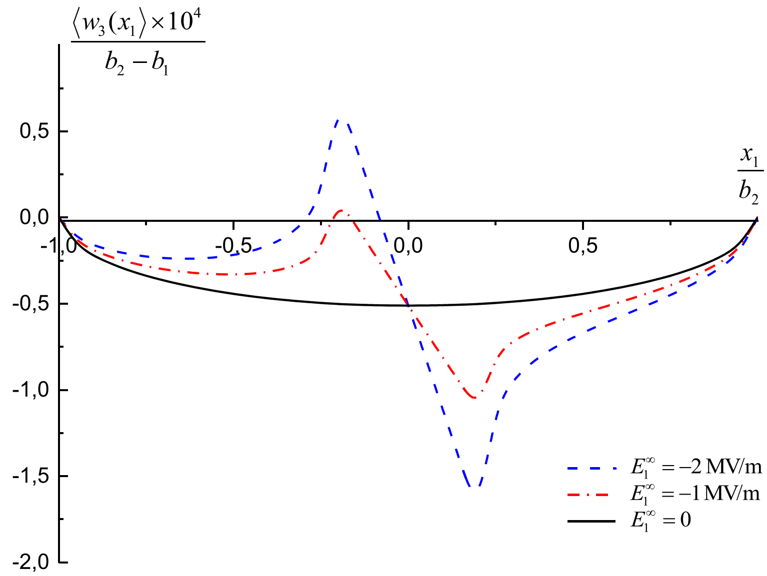

Fig. 3 The variation of the sliding displacement jump $\langle w_3(x_1)\rangle$ of the normalized phason crack faces along the crack region for different values of E_1^∞

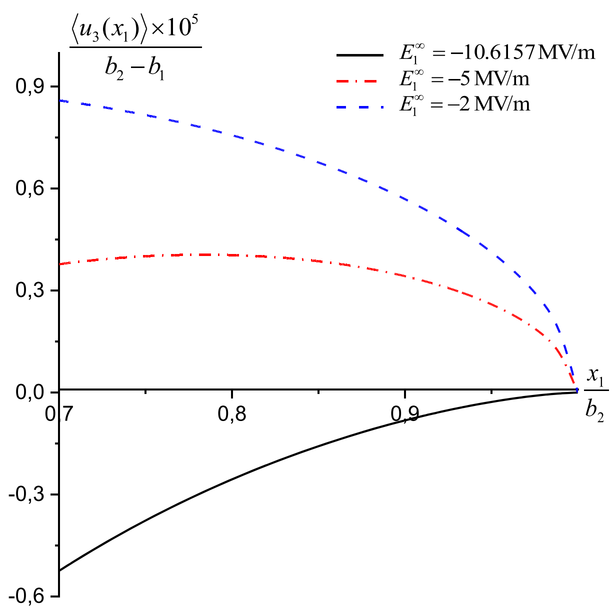

Fig. 4 The variation of the sliding displacement jump $\langle u_3(x_1)\rangle$ of the normalized phonon crack faces in the left neighboring area of the crack tip b_2 for different values of E_1^∞

$E_1^\infty = -10.6157$ MV/m in this figure corresponds to the external electrical loading for which $k_u = 0$. For this, Eq. (44) has been solved. It can be seen that for above-mentioned electrical loading the crack closes smoothly at its tip b_2, while for the two other cases a singularity is found at this point and the crack closes abruptly.

Figure 5 displays the effect of the length of the electrically permeable zones on the crack faces sliding displacement jump for the phonon field under the different parameter ϑ_1, where $\vartheta_2 = 0.4$, $E_1^\infty = -2$ MV/m. It can be seen that the phonon crack faces sliding displacement jump $\langle u_3(x_1)\rangle$ varies essentially with respect to the geometrical parameters ϑ_1 and ϑ_2. In addition, it follows from the presented results that the curves for the case of two electrically permeable crack face zones tend to the curves of an interface crack with one electrically permeable crack face zone while ϑ_1 tends to zero. Moreover, with further approach of a_1 toward

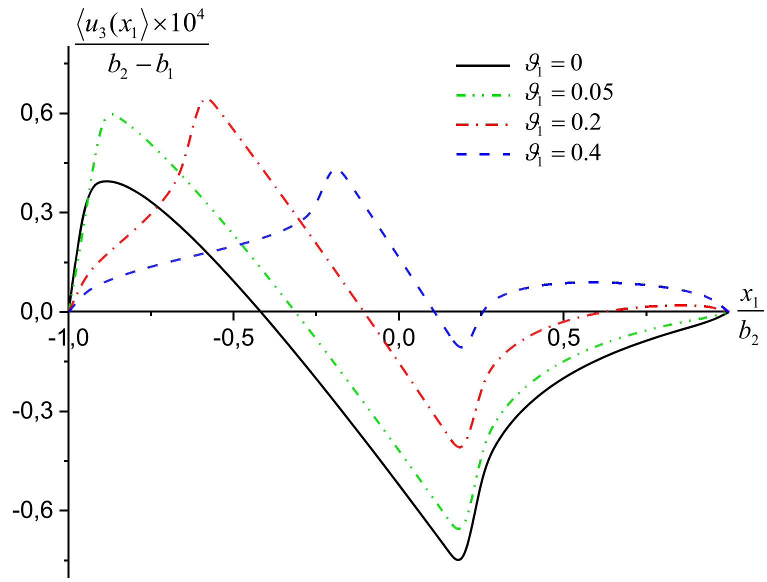

Fig. 5 The variation of the sliding displacement jump $\langle u_3(x_1)\rangle$ of the normalized phonon crack faces along the crack region for different values of ϑ_1

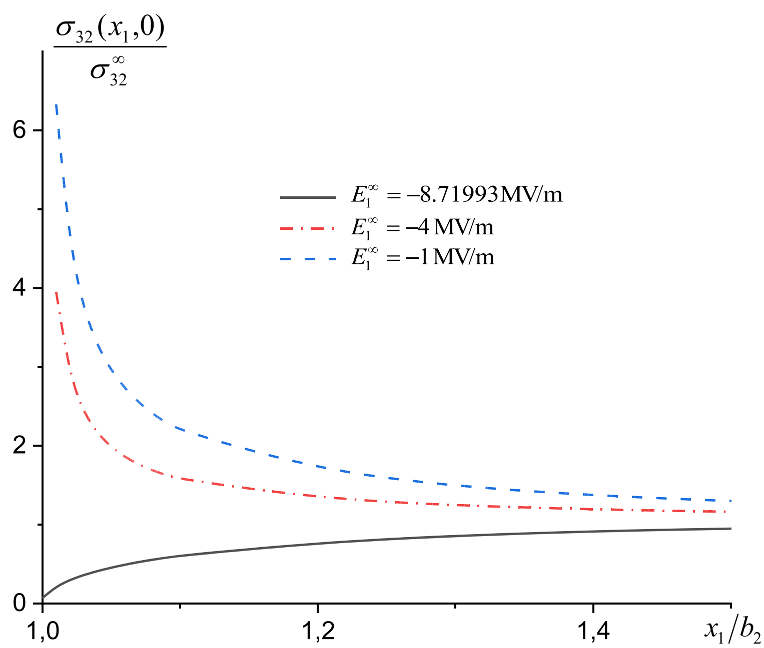

Fig. 6 Variation of the normalized phonon stress $\sigma_{32}(x_1, 0)$ along the crack continuation $x_1 > b_2$ for different values of E_1^{∞}

b_1, the corresponding curves completely coincide and the present results can be reduced to the degenerated case of the mixed electrical conditions at crack faces, which was considered by Loboda et al. [44].

Figure 6 shows the variations of the phonon stress $\sigma_{32}(x_1, 0)$ at the crack continuation $x_1 > b_2$ for different values of electric loading and $\vartheta_1 = \vartheta_2 = 0.4$. It is clearly observed from this figure that the phonon stress $\sigma_{32}(x_1, 0)$ is singular near the crack tip and tends to its nominal value for all x_1 being much larger than the crack length. The value $E_1^{\infty} = -8.71993$ MV/m in this figure corresponds to the external electrical loading for which $K_{\sigma}^{b_2} = 0$.

Figures 7 and 8 show the coupling effect between the phonon and phason fields. Numerical results are obtained for the same geometrical characteristics as before and $E_1^{\infty} = -2$ MV/m. Solid lines correspond to

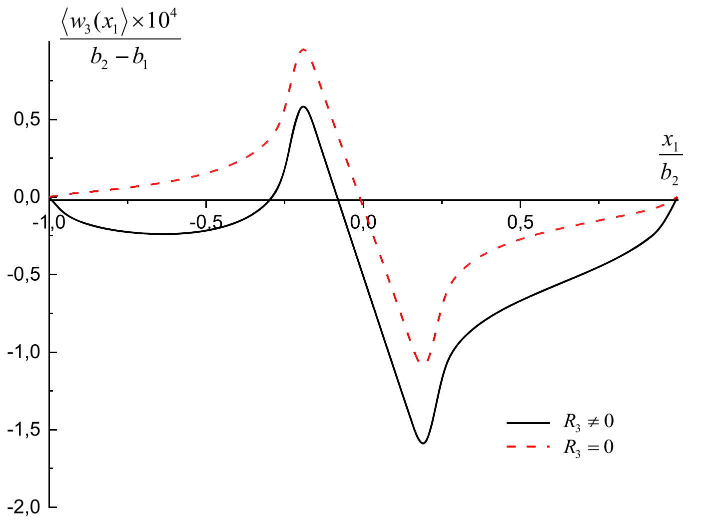

Fig. 7 The variation of the sliding displacement jump $\langle w_3(x_1)\rangle$ of the normalized phason crack faces along the crack region for different coupling constants

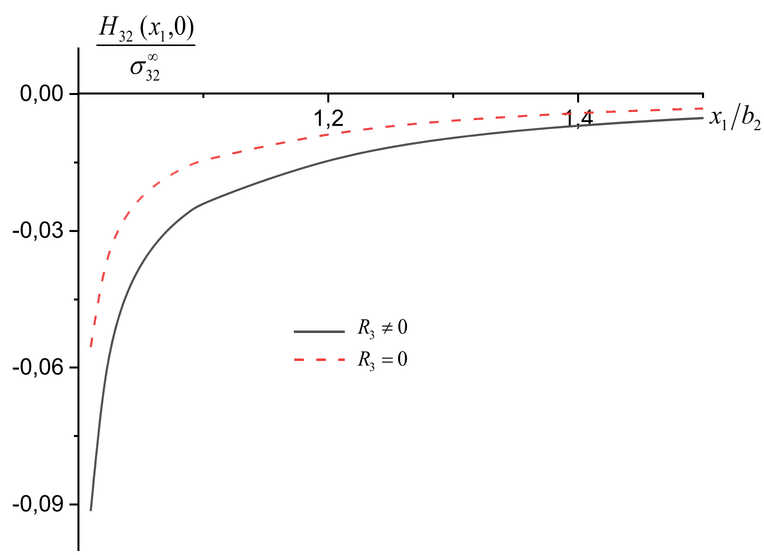

Fig. 8 Variation of the normalized phason stress $H_{32}(x_1, 0)$ along the crack continuation $x_1 > b_2$ for different coupling constants

the complete analysis of the problem in which the phonon–phason coupling effect is taken into account, and dashed lines show the results obtained by using the assumption of omitted coupling effect between phonon and phason fields, i.e., $R_3 = 0$. It follows from the numerical analysis that the coupling effect has strong influence on the phason displacement and stress. However, its influence on the phonon displacement and stress is rather weak. This phenomenon can be explained by consideration of only phonon loading in our problem.

The values of the mechanical and electrical intensity factors for $\vartheta_1 = \vartheta_2 = 0.4$ and different values of external electric loading E_1^{∞} are presented in Table 2. It can be seen that the dependence of all intensity factors on the external electric loading is rather essential. Moreover, due to certain values of the electric loading, each intensity factor can be made equal to zero. For example, the values $E_1^{\infty} = 2190.1$ V/m and $E_1^{\infty} = -7.07318$ MV/m in Table 2 correspond to the external electrical loading for which $K_E^{a_2} = 0$ and $K_E^{b_2} = 0$, respectively. This means that tuning of E_1^{∞} to the above mentioned values lead to removing the singularity in the electric field at the points a_2 and b_2, respectively, and decreases the danger of the crack development.

Table 2 The values of the intensity factors for different values of E_1^{∞}

E_1^{∞}[V/m]	$K_{\sigma}^{b_2}$[N/m$^{3/2}$]	$K_{H}^{b_2}$[N/m$^{3/2}$]	$K_{E}^{a_2}$[V/m$^{1/2}$]	$K_{E}^{b_2}$[V/m$^{1/2}$]	k_u[m$^{1/2}$]
-1×10^8	-1.855×10^6	-1.173×10^5	-7.915×10^6	5.015×10^4	1.969×10^{-5}
-1.06157×10^7	-3.853×10^4	-1.245×10^4	-8.404×10^5	1.911×10^3	≈ 0
-1×10^7	-2.602×10^4	-1.173×10^4	-7.916×10^5	1.580×10^3	-1.356×10^{-7}
-8.71993×10^6	≈ 0	-1.023×10^4	-6.903×10^5	8.887×10^2	-4.176×10^{-7}
-7.07318×10^6	3.347×10^4	-8.294×10^3	-5.600×10^5	≈ 0	-7.803×10^{-7}
-1×10^6	1.569×10^5	-1.173×10^3	-7.932×10^4	-3.278×10^3	-2.118×10^{-6}
-1×10^4	1.770×10^5	-11.86	-9.648×10^2	-3.812×10^3	-2.336×10^{-6}
-1×10^2	1.772×10^5	-0.247	-1.813×10^2	-3.817×10^3	-2.338×10^{-6}
0	1.772×10^5	-0.130	-1.733×10^2	-3.817×10^3	-2.338×10^{-6}
1.10621×10^2	1.773×10^5	≈ 0	-1.646×10^2	-3.817×10^3	-2.338×10^{-6}
2.1901×10^3	1.773×10^5	2.438	≈ 0	-3.818×10^3	-2.339×10^{-6}
1×10^4	1.775×10^5	11.596	6.181×10^2	-3.823×10^3	-2.341×10^{-6}

6 Conclusion

An interface crack between two dissimilar one-dimensional hexagonal piezoelectric quasicrystalline half-spaces under the action of anti-plane mechanical and in-plane electric loadings is considered. Mixed electric conditions at the crack faces are studied. It is assumed that the atom arrangement is periodic in the $(x_1,\ x_2)$-plane and quasiperiodic in the direction normal to this plane, while the positive x_3-axis represents also the direction of polarization.

Due to a special transformation of the matrix–vector representations (10), (11) of the field variables via analytical functions, the new representations (19), (20) convenient for the solution of the considered problem are found. On the basis of these representations, the problem is reduced to the homogeneous combined Dirichlet–Riemann problem (28), (29) and to the Hilbert problem (30) with the conditions (31), (32) at infinity, respectively. An exact analytical solution of these problems has been found, and analytical expressions for the phonon and phason stresses and the electric field as well as for the derivative jumps of the phonon and phason displacements and the electrical displacement jump along the bimaterial interface have been derived. It is shown that the obtained solution has a conventional square root singularity at the singular points. Taking this type of singularity into account, the mechanical and electrical intensity factors related to the singular points a_2 and b_2 have been determined.

The correctness of the obtained solution is confirmed by its comparison with the well-known solution for the degenerated case of the mixed electrical conditions at crack faces. The variations of the phonon and phason crack faces sliding displacements and the phonon stress along the corresponding parts of the material interface are illustrated in a graphical form for different values of the external electric loading. Furthermore, the mechanical and electrical intensity factors are presented in Table 2. It follows from the obtained results that the mechanical and electrical intensity factors essentially depend on the magnitude and direction of the applied external electric field and, moreover, each intensity factors can be set to zero by appropriate choosing of the mentioned field. The same can be found concerning the smoothing of the crack tip closure. This means that the crack propagation can either be enhanced or retarded depending on the electric loadings. Besides, the maximum of the phonon and phason crack faces sliding displacements increases as the external electric field increases. It is worth to be mentioned finally that the importance of the obtained analytical solution is enhanced by the possibility of using the derived equations and results for the prediction of the numerical solutions behavior at singular points for similar problems in finite-sized domains.

Acknowledgements The Author V. Govorukha would like to express his gratitude for the support of the Alexander von Humboldt Foundation through a Digital Cooperation Fellowship.

Author contributions V.G. and M.K. wrote the main manuscript text and V.G. prepared figures 1-6. All authors reviewed the manuscript

Declarations

Competing interests The authors declare no competing interests.

Appendix A

Consider a bimaterial compound, which consists of two piezoelectric quasicrystalline half-spaces $x_2 > 0$ and $x_2 < 0$ of different material properties. We assume, that the stresses of the phonon and phason fields, and the tangential component of the electric field are continuous across the whole bimaterial interface. This means that the boundary conditions in the plane $x_2 = 0$ are

$$\langle \sigma_{32}(x_1) \rangle = 0, \quad \langle H_{32}(x_1) \rangle = 0, \quad \langle E_1(x_1) \rangle = 0, \quad \text{for } x_1 \in (-\infty, \infty). \tag{A1}$$

To construct the representations, which satisfy the interface conditions, we use Eqs. (10) and (11) for the upper ($m = 1$) and lower ($m = 2$) half-spaces, which can be written in the form

$$\mathbf{v}^{(m)} = \mathbf{M}^{(m)} \mathbf{f}'^{(m)}(z) + \bar{\boldsymbol{M}}^{(m)} \bar{\boldsymbol{f}}'^{(m)}(\bar{z}) \tag{A2}$$

$$\mathbf{p}^{(m)} = \mathbf{N}^{(m)} \mathbf{f}'^{(m)}(z) + \bar{\boldsymbol{N}}^{(m)} \bar{\boldsymbol{f}}'^{(m)}(\bar{z}), \tag{A3}$$

where the arbitrary vector-functions $\mathbf{f}^{(1)}(z)$ and $\mathbf{f}^{(2)}(z)$ are analytic in the upper and the lower half-spaces, respectively.

According to the interface conditions (A1) and the relations (A3), we get

$$\mathbf{N}^{(1)} \mathbf{f}'^{(1)}(x_1 + i0) - \bar{\boldsymbol{N}}^{(2)} \bar{\boldsymbol{f}}'^{(2)} = N^{(2)} f'^{(2)}(x_1 - i0) - \bar{N}^{(1)} \bar{f}'^{(1)}(x_1 - i0) \text{ for } x_1 \in (-\infty, \infty) \tag{A4}$$

The left-hand side of equation (A4) is the boundary value of a vector-function being analytic in the domain $x_2 > 0$, and the right-hand side of this equation is the boundary value of another vector-function being analytic in the domain $x_2 < 0$. Hence, both vector-functions can be analytically continued into the whole complex plane, i.e., they are equal to an arbitrary vector-function, defined as

$$\mathbf{J}(z) = \begin{cases} \mathbf{N}^{(1)} \mathbf{f}'^{(1)}(z) - \bar{\mathbf{N}}^{(2)} \bar{\mathbf{f}}'^{(2)}(z) \text{ for } x_2 > 0 \\ \mathbf{N}^{(2)} \mathbf{f}'^{(2)}(z) - \bar{\mathbf{N}}^{(1)} \bar{\mathbf{f}}'^{(1)}(z) \text{ for } x_2 < 0 \end{cases}, \tag{A5}$$

which is analytic in the whole complex plane, including points along all bimaterial interface.

Taking into account that the phonon and phason stresses and the electric field are bonded at infinity, it follows from equation (A3) that $\mathbf{J}(\infty) = \mathbf{J}^{\infty}$, where $\mathbf{J}^{\infty}$ is a constant vector. But according to Liouville's theorem, this means that $\mathbf{J}(z) = \mathbf{J}^{\infty}$ holds true in the whole complex plane. Thus from equation (A5) it follows

$$\begin{aligned} \bar{\mathbf{f}}'^{(2)}(z) &= \left(\overline{N}^{(2)}\right)^{-1} N^{(1)} \mathbf{f}'^{(1)}(z) - \left(\overline{N}^{(2)}\right)^{-1} J^{\infty} \text{ for } x_2 > 0, \\ \mathbf{f}'^{(2)}(z) &= \left(N^{(2)}\right)^{-1} \overline{N}^{(1)} \bar{\boldsymbol{f}}'^{(1)}(z) - \left(N^{(2)}\right)^{-1} J^{\infty} \text{ for } x_2 < 0. \end{aligned} \tag{A6}$$

Since $f'^{(1)}(z)$ and $f'^{(2)}(z)$ are arbitrary functions, one can set $J^{\infty} = \begin{bmatrix} 0 \ 0 \ 0 \end{bmatrix}^T$, and equations (A6) get the form

$$\begin{aligned} \bar{\mathbf{f}}'^{(2)}(z) &= \left(\overline{N}^{(2)}\right)^{-1} N^{(1)} \mathbf{f}'^{(1)}(z) \text{ for } x_2 > 0, \\ \mathbf{f}'^{(2)}(z) &= \left(N^{(2)}\right)^{-1} \overline{N}^{(1)} \bar{\mathbf{f}}'^{(1)}(z) \text{ for } x_2 < 0. \end{aligned} \tag{A7}$$

Consider further the expressions

$$\langle v(x_1) \rangle = v^{(1)}(x_1 + i0) - v^{(2)}(x_1 - i0)$$

for the derivatives of the jumps of phonon and phason displacements and electrical displacement jump over the bimaterial interface, which, in view of (A2) and (A7), takes the form

$$\langle v(x_1) \rangle = \mathbf{D} \mathbf{f}'^{(1)}(x_1) + \bar{\mathbf{D}} \bar{\mathbf{f}}'^{(1)},$$

where $\mathbf{D} = \mathbf{M}^{(1)} - \bar{\boldsymbol{M}}^{(2)} \left(\bar{\boldsymbol{N}}^{(2)}\right)^{-1} \mathbf{N}^{(1)}$.

Furthermore, we assume that the part L of the bimaterial interface is mechanically and electrically bounded, i.e., the boundary conditions at this part of the bimaterial interface are or

$$\langle v(x_1)\rangle = 0 \text{ for } x_1 \in L$$

$$\mathbf{D} = \mathbf{M}^{(1)}(x_1) = -\bar{\mathbf{D}}\bar{\mathbf{f}}'^{(1)}(x_1) \text{ for } x_1 \in L. \tag{A8}$$

Continuity of the phonon and phason displacements and the electrical displacement across the bonded bimaterial interface, as inferred from (A8), implies that an arbitrary vector-function defined as

$$\mathbf{W}(z) = \begin{cases} \mathbf{D}\mathbf{f}'^{(1)}(z) \text{ for } x_2 > 0 \\ -\bar{\mathbf{D}}\bar{\mathbf{f}}'^{(1)}(z) \text{ for } x_2 < 0 \end{cases}$$

is analytic in the whole complex plane cut along $(-\infty,\ \infty)\backslash L$. Then, the field variables at the bimaterial interface can be expressed via the boundary values of the function $\mathbf{W}$(z) in such a way that

$$\langle v(x_1)\rangle = \mathbf{W}^{+}(x_1) - \mathbf{W}^{-}(x_1), \tag{A9}$$

$$\mathbf{p}(x_1, 0) = \mathbf{G}\mathbf{W}^{+}(x_1) - \bar{\boldsymbol{G}}\boldsymbol{W}^{-}(x_1), \tag{A10}$$

where $\mathbf{G} = \mathbf{N}^{(1)}(\mathbf{D})^{-1}$ and the superscripts ‘ + ’ and ‘−‘ indicate the limit values at the bimaterial interface taken from the upper and the lower half-spaces, respectively.

Equations (A9) and (A10) can be used for the analysis of a bimaterial compound, which consists of dissimilar one-dimensional hexagonal piezoelectric QCs with cracks at their bimaterial interface.

Appendix B

The general solution of the homogeneous combined Dirichlet–Riemann boundary value problem (28) and (29) can be presented in the form [41]

$$\Phi_1(z) = X(z)[P(z) + iY(z)Q(z)], \tag{B1}$$

where

$$X(z) = \frac{e^{i\phi(z)}}{(z-d)\sqrt{(z-a_1)(z-a_2)}},\ \ Y(z) = \sqrt{\frac{(z-a_1)(z-a_2)}{(z-b_1)(z-b_2)}},$$

$$\phi(z) = -Z(z)\left(\varepsilon_1\int_{a_1}^{a_2}\frac{\mathrm{d}t}{Z^{+}(t)(t-z)} + i\int_{b_1}^{a_1}\frac{h_1(t)\mathrm{d}t}{Z^{+}(t)(t-z)} + i\int_{a_2}^{b_2}\frac{h_2(t)\mathrm{d}t}{Z^{+}(t)(t-z)}\right),\ \ \varepsilon_1 = \frac{\ln\gamma_1}{2\pi},$$

$$Z(z) = \sqrt{(z-a_1)(z-a_2)(z-b_1)(z-b_2)},\ \ h_1(x_1) = n^*,\ \ h_2(x_1) = \begin{cases} 1,\ x_1 \in (a_2,\ d) \\ 0,\ x_1 \in (d,\ b_2) \end{cases},$$

n^* is an integer, and $d \in (a_2,\ b_2)$ is an unknown pole of the function $X(z)$.

The function $\varphi(z)$ can be represented via elliptic integrals as

$$\phi(z) = \frac{-2}{\sqrt{(b_2-a_1)(a_2-b_1)}}\left\{\varepsilon_1\sqrt{\frac{(z-a_2)(z-b_2)}{(z-a_1)(z-b_1)}}\varphi_1(z) + \right.$$
$$\left. + n^*\sqrt{\frac{(z-a_1)(z-a_2)}{(z-b_1)(z-b_2)}}\varphi_2(z) - \sqrt{\frac{(z-b_1)(z-b_2)}{(z-a_1)(z-a_2)}}\varphi_3(z)\right\},$$

where

$$\phi_1(z) = (a_1-b_1)\Pi(p_1,\ q) + (z-a_1)K(q),\ \ p_1 = p_1^*\frac{z-b_1}{z-a_1},\ \ p_1^* = \frac{a_2-a_1}{a_2-b_1},$$

$$\phi_2(z) = (b_1-b_2)\Pi(p_2,\ r) + (z-b_1)K(r),\ \ p_2 = p_2^*\frac{z-b_2}{z-b_1},\ \ p_2^* = \frac{b_1-a_1}{b_2-a_1},$$

$$\phi_3(z) = (a_2-a_1)\Pi(\mu,\ p_3,\ r) + (z-a_2)F(\mu,\ r),\ \ p_3 = p_3^*\frac{z-a_1}{z-a_2},\ \ p_3^* = \frac{b_2-a_2}{b_2-a_1},$$

$q = \sqrt{\frac{(a_2-a_1)(b_2-b_1)}{(b_2-a_1)(a_2-b_1)}}$, $r = \sqrt{\frac{(b_2-a_2)(a_1-b_1)}{(b_2-a_1)(a_2-b_1)}}$, $\mu = \arcsin\sqrt{\frac{(b_2-a_1)(d-a_2)}{(b_2-a_2)(d-a_1)}}$. Here $F(\mu, r)$ and $\Pi(\mu, p, r)$ are incomplete elliptic integrals of the first and third kind, while $K(r)$ and $\Pi(p, r)$ are complete elliptic integrals of the first and third kind.

The expansion of the function $\varphi(z)$ at infinity has the form

$$\varphi(z)|_{z\to\infty} = A_1 z + (A_2 + \xi_1 A_1) + (A_3 + \xi_1 A_2 + \xi_2 A_1)z^{-1} + O\left(z^{-2}\right),$$

where

$$A_j = \varepsilon_1 \int_{a_1}^{a_2} \frac{t^{j-1}\mathrm{d}t}{Z(t)} + i\int_{b_1}^{a_1} \frac{t^{j-1}h_1(t)\mathrm{d}t}{Z^+(t)} + i\int_{a_2}^{b_2} \frac{t^{j-1}h_2(t)\mathrm{d}t}{Z^+(t)}, \quad j = 1, 2, 3.$$

The integer n^* and the pole d can be found from the condition of finite values at infinity of the function $\varphi(z)$ as

$$-\varepsilon_1\frac{K(q)}{K(r)} < n^* < 1 - \varepsilon_1\frac{K(q)}{K(r)}$$

$d = \frac{a_1(b_2-a_2)sn^2(\omega, r)-a_2(b_2-a_1)}{(b_2-a_2)sn^2(\omega, r)-(b_2-a_1)}$

where $sn(\omega, r)$ is the Jacobi elliptic function and $\omega = \varepsilon_1 K(q) + n^* K(r)$.

The polynomials $P(z)$ and $Q(z)$, appearing in the solution (B1), have the form

$$P(z) = C_0 + C_1 z + C_2 z^2, \quad Q(z) = D_0 + D_1 z + D_2 z^2,$$

where the coefficients

$$C_0 = -C_1\left(d - \frac{\chi}{\chi^*}\right) - \mathrm{d}C_2\left(d - \frac{2\chi}{\chi^*}\right) - \frac{\chi^2}{\chi^*}(D_1 + 2\mathrm{d}D_2),$$
$$D_0 = \frac{1}{\chi^*}(C_1 + 2\mathrm{d}C_2) - D_1\left(d + \frac{\chi}{\chi^*}\right) - \mathrm{d}D_2\left(d + \frac{2\chi}{\chi^*}\right),$$
$$C_1 = \alpha_1 D_2 - \nu_1 C_2,$$
$$D_1 = -(\nu_1 + \eta_1)D_2 - \alpha_1 C_2,$$
$$C_2 = \frac{h_{13}E_1^\infty}{1+\gamma_1}\cos\alpha_0 + \frac{-h_{11}\sigma_{32}^\infty - H_{32}^\infty}{1+\gamma_1}\sin\alpha_0,$$
$$D_2 = \frac{-h_{11}\sigma_{32}^\infty - H_{32}^\infty}{1+\gamma_1}\cos\alpha_0 - \frac{h_{13}E_1^\infty}{1+\gamma_1}\sin\alpha_0$$

are determined by the condition at infinity (31) for the function $\Phi_1(z)$ as well as the condition of the phonon and phason displacement uniqueness and the absence of an electric charge in the crack region. In the above formulas

$$\chi = \sqrt{\frac{(d-a_1)(d-a_2)}{(d-b_1)(b_2-d)}},$$
$$\chi^* = \frac{1}{2\chi}\left[\frac{(2d-a_1-a_2)(d-b_1)(b_2-d) + (2d-b_1-b_2)(d-a_1)(d-a_2)}{(d-b_1)^2(b_2-d)^2}\right],$$
$$\eta_1 = -\frac{1}{2}(a_1+a_2-b_1-b_2), \quad \nu_1 = \frac{a_1+a_2}{2} + d, \quad \alpha_0 = A_2, \quad \alpha_1 = A_3 + \xi_1 A_2.$$

Further, taking into account the expression $F_1(z) = i\Phi_1(z)$, we get

$$F_1(z) = iX(z)[P(z) + iY(z)Q(z)]. \tag{B2}$$

References

1. Shechtman, D., Blech, I., Gratias, D., Cahn, J.W.: Metallic phase with long-range orientational order and no translational symmetry. Phys. Rev. Lett. **53**, 1951–1953 (1984)
2. Elina, H.S.: Microstructure, fabrication and properties of quasicrystalline Al-Cu-Fe alloys: a review. J. Alloy. Compd. **363**, 154–178 (2004)
3. Bak, P.: Phenomenological theory of icosahedral incommensurate (‘quasiperiodic’) order in Mn–Al alloys. Phys. Rev. Lett. **54**, 1517–1519 (1985)
4. Steurer, W., Deloudi, S.: Crystallography of Quasicrystals: Concepts, Methods and Structures. Springer, Berlin, Heidelberg (2009)
5. Ding, D.H., Yang, W.G., Hu, C.Z., Wang, R.H.: Generalized elasticity theory of quasicrystals. Phys. Rev. B **48**, 7003–7010 (1993)
6. Hu, C.Z., Wang, R.H., Ding, D.H.: Symmetry groups, physical property tensors, elasticity and dislocations in quasicrystals. Rep. Prog. Phys. **63**, 1–39 (2000)
7. Fan, T.Y., Mai, Y.W.: Elasticity theory, fracture mechanics and some relevant thermal properties of quasi-crystalline materials. Appl. Mech. Rev. **57**, 325–343 (2004)
8. Fujiwara, T., Ishii, Y. (eds.): Quasicrystals. Handbook of Metal Physics. Elsevier, Amsterdam (2008)
9. Suck, J.-B., Schreiber, M., Haussler, P. (eds.): Quasicrystals: An Introduction to Structure. Physical Properties and Applications. Springer, Berlin (2010)
10. Fan, T.Y.: Mathematical Theory of Elasticity of Quasicrystals and its Applications. Springer, Beijing (2011)
11. Hu, C.Z., Wang, R.H., Ding, D.H., Yang, W.G.: Piezoelectric effects in quasicrystals. Phys. Rev. B **56**, 2463–2468 (1997)
12. Altay, G., Dömeci, M.C.: On the fundamental equations of piezoelasticity of quasicrystal media. Int. J. Solids Struct. **49**, 3255–3262 (2012)
13. Li, C.-L., Liu, Y.-Y.: The physical property tensors of one-dimensional quasicrystals. Chin. Phys. **13**, 924–931 (2004)
14. Rao, K.R.M., Rao, P.H., Chaitanya, B.S.K.: Piezoelectricity in quasicrystals: a group-theoretical study. Pramana J. Phys. **68**, 481–487 (2007)
15. Zhang, L., Wu, D., Xu, W., Yang, L., Ricoeur, A., Wang, Z., Gao, Y.: Green’s functions of one-dimensional quasicrystal bi-material with piezoelectric effect. Phys. Lett. A **380**, 3222–3228 (2016)
16. Li, X.Y., Li, P.D., Wu, T.H., Shi, M.X., Zhu, Z.W.: Three-dimensional fundamental solutions for one-dimensional hexagonal quasicrystal with piezoelectric effect. Phys. Lett. A **378**, 826–834 (2014)
17. Li, X.Y., Wang, T., Zheng, R.F., Kang, G.Z.: Fundamental thermo-electro-elastic solutions for 1D hexagonal QC. Z. Angew. Math. Mech. **95**, 457–468 (2015)
18. Zhang, L.L., Zhang, Y.M., Gao, Y.: General solutions of plane elasticity of one-dimensional orthorhombic quasicrystals with piezoelectric effect. Phys. Lett. A **378**, 2768–2776 (2014)
19. Xu, W.S., Wu, D., Gao, Y.: Fundamental elastic field in an infinite plane of two dimensional piezoelectric quasicrystal subjected to multi-physics loads. Appl. Math. Model. **52**, 186–196 (2017)
20. Guo, J.H., Pan, E.N.: Three-phase cylinder model of one-dimensional hexagonal piezoelectric quasi-crystal composites. J. Appl. Mech. **83**, 081007–081010 (2016)
21. Fan, C.Y., Li, Y., Xu, G.T., Zhao, M.H.: Fundamental solutions and analysis of three-dimensional cracks in one-dimensional hexagonal piezoelectric quasicrystals. Mech. Res. Commun. **74**, 39–44 (2016)
22. Zhou, Y.B., Li, X.F.: Fracture analysis of an infinite 1D hexagonal piezoelectric quasicrystal plate with a penny-shaped dielectric crack. Eur. J. Mech. A. Solids **76**, 224–234 (2019)
23. Yu, J., Guo, J.H., Pan, E., Xing, Y.M.: General solutions of plane problem in one-dimensional quasicrystal piezoelectric materials and its application on fracture mechanics. Appl. Math. Mech. Engl. Ed. **36**, 793–814 (2015)
24. Zhou, Y.B., Li, X.F.: Two collinear mode-III cracks in one-dimensional hexagonal piezoelectric quasicrystal strip. Eng. Fract. Mech. **189**, 133–147 (2018)
25. Zhou, Y.B., Li, X.F.: Exact solution of two collinear cracks normal to the boundaries of a 1D layered hexagonal piezoelectric quasicrystal. Philos. Mag. **98**, 1780–1798 (2018)
26. Yang, J., Li, X.: The anti-plane shear problem of two symmetric cracks originating from an elliptical hole in 1D hexagonal piezoelectric QCs. Adv. Mater. Res. **936**, 127–135 (2014)
27. Yang, J., Li, X.: Analytic solutions of problem about a circular hole with a straight crack in one-dimensional hexagonal quasicrystals with piezoelectric effects. Theor. Appl. Fract. Mech. **82**, 17–24 (2016)
28. Yang, J., Zhou, Y.T., Ma, H.L., Ding, S.H., Li, X.: The fracture behavior of two asymmetrical limited permeable cracks emanating from an elliptical hole in one-dimensional hexagonal quasicrystals with piezoelectric effect. Int. J. Solids Struct. **108**, 175–185 (2017)
29. Zhou, Y.B., Li, X.F.: A Yoffe-type moving crack in one-dimensional hexagonal piezoelectric quasicrystals. Appl. Math. Model. **65**, 148–163 (2019)
30. Tupholme, G.E.: One-dimensional piezoelectric quasicrystals with an embedded moving, non-uniformly loaded shear crack. Acta Mech. **228**, 547–560 (2017)
31. Tupholme, G.E.: A non-uniformly loaded anti-plane crack embedded in a half-space of a one-dimensional piezoelectric quasicrystal. Meccanica **53**, 973–983 (2018)
32. Zhao, M.H., Dang, H.Y., Fan, C.Y., Chen, Z.T.: Analysis of a three-dimensional arbitrarily shaped interface crack in a one-dimensional hexagonal thermo-electro-elastic quasicrystal bi-material. Part 1: Theoretical solution. Eng. Fract. Mech. **179**, 59–78 (2017)
33. Dang, H.Y., Zhao, M.H., Fan, C.Y., Chen, Z.T.: Analysis of a three-dimensional arbitrarily shaped interface crack in a one-dimensional hexagonal thermo-electro-elastic quasicrystal bi-material. Part 2: Numerical method. Eng. Fract. Mech. **180**, 268–281 (2017)
34. Hu, K.Q., Jin, H., Yang, Z., Chen, X.: Interface crack between dissimilar one-dimensional hexagonal quasicrystals with piezoelectric effect. Acta Mech. **230**, 2455–2474 (2019)

35. Loboda, V., Komarov, O., Bilyi, D., Lapusta, Y.: An analytical approach to the analysis of an electrically permeable interface crack in a 1-D piezoelectric quasicrystal. Acta Mech. **231**, 3419–3433 (2020)
36. Hu, K.Q., Gao, C., Zhong, Z., Chen, Z.: Interaction of collinear interface cracks between dissimilar one-dimensional hexagonal piezoelectric quasicrystals. Z. Angew. Math. Mech. **101**, e202000360 (2021)
37. Beom, H.G., Atluri, S.N.: Conducting cracks in dissimilar piezoelectric media. Int. J. Fract. **118**, 285–301 (2002)
38. Loboda, V., Sheveleva, A., Lapusta, Y.: An electrically conducting interface crack with a contact zone in a piezoelectric bimaterial. Int. J. Solids Struct. **51**, 63–73 (2014)
39. Onopriienko, O., Loboda, V., Sheveleva, A., Lapusta, Y.: Bond zone model for a conductive crack at the interface of piezoelectric materials under anti-plane mechanical and in-plane electric loadings. Z. Angew. Math. Mech. **99**, e201800230 (2019)
40. Nakhmein, E.L., Nuller, B.M.: The pressure of a system of stamps on an elastic half-plane under general conditions of contact adhesion and slip. J. Appl. Math. Mech. **52**, 223–230 (1988)
41. Govorukha, V., Kamlah, M., Loboda, V., Lapusta, Y.: An electrically permeable crack between two different piezoelectric materials. In: Wriggers, P., Eberhard, P. (eds.) Fracture Mechanics of Piezoelectric Solids with Interface Cracks. Lecture Notes in Applied and Computational Mechanics, vol. 83, pp. 59–95. Springer, Berlin (2017)
42. Muskhelishvili, N.I.: Some Basic Problems in the Mathematical Theory of Elasticity. Noordhoff, Groningen (1953)
43. Muskhelisvili, N.I.: Singular integral equations. Noordhoff, Groningen (1953)
44. Loboda, V., Sheveleva, A., Komarov, O., Lapusta, Y.: An interface crack with mixed electrical conditions at it faces in 1D quasicrystal with piezoelectric effect. Mech. Adv. Mater. Struct. **29**, 3334–3344 (2022)